

Improving the Foundation Layers for Concrete Pavements

TECHNICAL REPORT:

Field Evaluation of Premature Pavement Joint Deterioration – Iowa Urbandale Drive Field Study



December 2015

Sponsored by

Federal Highway Administration (DTFH 61-06-H-00011 (Work Plan #18))

FHWA TPF-5(183): California, Iowa (lead state), Michigan, Pennsylvania, Wisconsin

National Concrete Pavement
Technology Center



CENTER FOR

CEER

EARTHWORKS ENGINEERING
RESEARCH

IOWA STATE UNIVERSITY
Institute for Transportation

About the National CP Tech Center

The mission of the National Concrete Pavement Technology (CP Tech) Center is to unite key transportation stakeholders around the central goal of advancing concrete pavement technology through research, tech transfer, and technology implementation.

About CEER

The mission of the Center for Earthworks Engineering Research (CEER) at Iowa State University is to be the nation's premier institution for developing fundamental knowledge of earth mechanics, and creating innovative technologies, sensors, and systems to enable rapid, high quality, environmentally friendly, and economical construction of roadways, aviation runways, railroad embankments, dams, structural foundations, fortifications constructed from earth materials, and related geotechnical applications.

Disclaimer Notice

The contents of this report reflect the views of the authors, who are responsible for the facts and the accuracy of the information presented herein. The opinions, findings and conclusions expressed in this publication are those of the authors and not necessarily those of the sponsors.

The sponsors assume no liability for the contents or use of the information contained in this document. This report does not constitute a standard, specification, or regulation.

The sponsors do not endorse products or manufacturers. Trademarks or manufacturers' names appear in this report only because they are considered essential to the objective of the document.

Iowa State University Non-Discrimination Statement

Iowa State University does not discriminate on the basis of race, color, age, ethnicity, religion, national origin, pregnancy, sexual orientation, gender identity, genetic information, sex, marital status, disability, or status as a U.S. veteran. Inquiries regarding non-discrimination policies may be directed to Office of Equal Opportunity, Title IX/ADA Coordinator, and Affirmative Action Officer, 3350 Beardshear Hall, Ames, Iowa 50011, 515-294-7612, email eooffice@iastate.edu.

Iowa Department of Transportation Statements

Federal and state laws prohibit employment and/or public accommodation discrimination on the basis of age, color, creed, disability, gender identity, national origin, pregnancy, race, religion, sex, sexual orientation or veteran's status. If you believe you have been discriminated against, please contact the Iowa Civil Rights Commission at 800-457-4416 or the Iowa Department of Transportation affirmative action officer. If you need accommodations because of a disability to access the Iowa Department of Transportation's services, contact the agency's affirmative action officer at 800-262-0003.

The preparation of this report was financed in part through funds provided by the Iowa Department of Transportation through its "Second Revised Agreement for the Management of Research Conducted by Iowa State University for the Iowa Department of Transportation" and its amendments.

The opinions, findings, and conclusions expressed in this publication are those of the authors and not necessarily those of the Iowa Department of Transportation or the U.S. Department of Transportation Federal Highway Administration.

Technical Report Documentation Page

1. Report No. DTFH 61-06-H-00011 Work Plan 18		2. Government Accession No.		3. Recipient's Catalog No.	
4. Title and Subtitle Improving the Foundation Layers for Pavements: Field Evaluation of Premature Pavement Joint Deterioration – Iowa Urbandale Drive Field Study				5. Report Date December 2015	
				6. Performing Organization Code	
7. Author(s) Pavana Vennapusa, Peter Taylor, David White				8. Performing Organization Report No. InTrans Project 09-352	
9. Performing Organization Name and Address National Concrete Pavement Technology Center and Center for Earthworks Engineering Research Iowa State University 2711 South Loop Drive, Suite 4700 Ames, IA 50010-8664				10. Work Unit No. (TRAIS)	
				11. Contract or Grant No.	
12. Sponsoring Organization Name and Address Federal Highway Administration U.S. Department of Transportation 1200 New Jersey Avenue SE Washington, DC 20590				13. Type of Report and Period Covered Technical Report	
				14. Sponsoring Agency Code TPF-5(183)	
15. Supplementary Notes Visit www.cptechcenter.org or www.ceer.iastate.edu for color PDF files of this and other research reports.					
16. Abstract This technical project report is one of the field project reports developed as part of the TPF-5(183) and FHWA DTFH 61-06-H-00011:WO18 studies. This report summarized field test results and observations of a forensic investigation conducted on north bound (NB) and south bound (SB) lanes of NW Urbandale Drive in Urbandale, Iowa, to assess the causes of premature joint distresses observed at transverse and longitudinal joints. The SB lanes showed significantly more premature joint distresses than the NB lanes. The site consisted of a four-lane divided roadway constructed in 1997 with 260 mm (10.2 in.) thick jointed PCC pavement supported over a nominal 150 mm (5.9 in.) thick special backfill subbase layer and compacted subgrade. The objectives of the field study were to assess the causes for premature joint failures on the roadway and investigate if there were any differences between the NB and SB lanes that contributed to higher distresses on the SB lanes than on the NB lanes. The field study involved conducting falling weight deflectometer (FWD) tests on selected panels on NB and SB lanes, pavement coring near joints and away from joints, and dynamic cone penetrometer (DCP) and core hole permeameter (CHP) tests at selected core locations. FWD tests were conducted to assess load transfer efficiency (LTE) of pavement joints, deflections under dynamic loading, voids beneath pavement, and modulus of subgrade reaction (<i>k</i>). CHP tests were conducted to assess in situ drainage conditions. Pavement cores were assessed for damage in situ and were then sent to laboratory for petrographic analysis. In summary, the main cause of premature joint deterioration related damage at this site is freeze/thaw distress occurring as a result of poor drainage in the joints, which resulted in trapped water. Increased saturation because of trapped water combined with a marginal air-void system at the surface and an elevated w/cm ratio significantly increased the risk of damage. Results obtained from NB and SB lanes did not provide conclusive evidence that there is difference between the two lanes in terms of support conditions or drainage conditions or concrete material properties.					
17. Key Words concrete pavement—pavement foundation—joint deterioration—permeability—stiffness—subbase—subgrade				18. Distribution Statement No restrictions.	
19. Security Classification (of this report) Unclassified.		20. Security Classification (of this page) Unclassified.		21. No. of Pages 48	22. Price NA

**IMPROVING THE FOUNDATION LAYERS
FOR CONCRETE PAVEMENTS:
FIELD EVALUATION OF PREMATURE PAVEMENT
JOINT DETERIORATION – IOWA URBANDALE DRIVE
FIELD STUDY**

Technical Report
December 2015

Research Team Members

Tom Cackler, David J. White, Jeffrey R. Roesler, Barry Christopher, Andrew Dawson,
Heath Gieselman, and Pavana Vennapusa

Report Authors

Pavana K. R. Vennapusa, Peter Taylor, David J. White
Iowa State University

Sponsored by

the Federal Highway Administration (FHWA)
DTFH61-06-H-00011 Work Plan 18
FHWA Pooled Fund Study TPF-5(183): California, Iowa (lead state),
Michigan, Pennsylvania, Wisconsin

Preparation of this report was financed in part
through funds provided by the Iowa Department of Transportation
through its Research Management Agreement with the
Institute for Transportation
(InTrans Project 09-352)

**National Concrete Pavement Technology Center and
Center for Earthworks Engineering Research**

Iowa State University
2711 South Loop Drive, Suite 4700
Ames, IA 50010-8664
Phone: 515-294-8103
www.cptechcenter.org and www.ceer.iastate.edu

TABLE OF CONTENTS

ACKNOWLEDGMENTS	ix
LIST OF ACRONYMS AND SYMBOLS	xi
EXECUTIVE SUMMARY	xiii
Core Samples	xiv
Pavement Support and Drainage Conditions	xiv
Recommendations	xiv
CHAPTER 1. INTRODUCTION	1
CHAPTER 2. BACKGROUND	2
Literature Review on Joint Deterioration	2
NW Urbandale Drive Project Information	4
CHAPTER 3. EXPERIMENTAL TEST METHODS	6
Laboratory Testing Methods	6
In Situ Testing Methods and Data Analysis	6
Dynamic Cone Penetrometer	6
Kuab Falling Weight Deflectometer	7
Core Hole Permeameter	13
CHAPTER 4. LABORATORY TEST RESULTS	16
CHAPTER 5. FIELD OBSERVATIONS AND TEST RESULTS	17
Description of Test Sections	17
Core Sample Observations	17
Field Test Results	22
CHAPTER 6. KEY FINDINGS AND RECOMMENDATIONS	28
Core Samples	28
Pavement Support and Drainage Conditions	28
Recommendations	29
REFERENCES	31

LIST OF FIGURES

Figure 1. Shadowing microcracking near joints (Taylor 2011).....	3
Figure 2. Petrographic examination of core sample taken from distressed joint with voids filled with ettringite at locations pointed with red arrows (Taylor et al. 2012).....	4
Figure 3. Map of NW Urbandale Drive between I-35/I-80 ramp south of the freeway bridge to Meredith Drive in Urbandale, Iowa, with approximate locations of the test sections.....	5
Figure 4. Photos of joint deterioration observed on NW Urbandale Drive in July-August 2013 (pictures courtesy of Gary Reed, P.E. from CDA)	5
Figure 5. Dynamic cone penetrometer testing	7
Figure 6. KUAB falling weight deflectometer (FWD).....	8
Figure 7. FWD deflection sensor setup used for this study and an example deflection basin.....	8
Figure 8. Void detection using load-deflection data from FWD test.....	9
Figure 9. Static k_{PLT} values versus $k_{FWD-Dynamic}$ measurements reported in literature	12
Figure 10. Core hole permeameter (CHP) device and components.....	13
Figure 11. Core hore permeability testing in situ on Urbandale Drive.....	14
Figure 12. Particle size distribution curves of subgrade and subbase layers	16
Figure 13. Core 4 on NB lane south of Plum Drive (TS2)	19
Figure 14. Core 5 on NB lane south of Plum Drive (TS2)	19
Figure 15. Core 6 on NB Lane south of Plum Drive (TS2).....	20
Figure 16. Core 7 on NB lane north of Plum Drive (TS3)	20
Figure 17. Core 8 on SB lane south of Plum Drive (TS4).....	21
Figure 18. Core 9 on SB lane south of Plum Drive (TS4).....	21
Figure 19. Core 10 on SB lane south of Plum Drive	22
Figure 20. FWD test results from TS1.....	23
Figure 21. FWD test results on TS2.....	24
Figure 22. FWD test results from TS4.....	25
Figure 23. DCP-CBR and cumulative blows with depth from three core locations (Cores 1, 5, and 9)	26
Figure 24. CHP test results from three core locations (Cores 1, 5, and 9)	27

LIST OF TABLES

Table 1. AASHTO (1993) drainage quality rating	15
Table 2. Recommended values of C_d for PCC pavement design (AASHTO 1993).....	15
Table 3. Summary of material index properties.....	16
Table 4. Summary of test sections and in situ testing.....	17
Table 5. Summary of core sample observations	18
Table 6. Summary of in situ test results.....	27

ACKNOWLEDGMENTS

This research was conducted under Federal Highway Administration (FHWA) DTFH61-06-H-00011 Work Plan 18 and the FHWA Pooled Fund Study TPF-5(183), involving the following state departments of transportation:

- California
- Iowa (lead state)
- Michigan
- Pennsylvania
- Wisconsin

The authors would like to express their gratitude to the National Concrete Pavement Technology (CP Tech) Center, the FHWA, the Iowa Department of Transportation (DOT), and the other pooled fund state partners for their financial support and technical assistance.

Mr. Gary Reed, P.E., with Civil Design Advantage provided access to the project site and background information on the project. Team Services, Inc., performed coring operations and CTL Group provided petrographic analysis test results. We greatly appreciate their help. Christianna White provided comments and editorial support.

LIST OF ACRONYMS AND SYMBOLS

CBR	California bearing ratio
C_d	Coefficient of drainage
CBR _{SG}	CBR of subgrade determined from DCP testing
CBR _{SB}	CBR of subbase determined from DCP testing
DPI	Dynamic penetration index
D_0	Deflection measured under the plate
D_0^*	Non-dimensional deflection coefficient
D_1	Deflection of the unloaded slab
D_1 to D_7	Deflections measured away from the plate at various set distances
I	Intercept
k	Modulus of subgrade reaction
k_{AASHTO}	Modulus of subgrade reaction determined following AASHTO (1993) procedure
K_{CHP}	Hydraulic conductivity determined from core hole permeameter testing
$k_{FWD-Dynamic}$	Dynamic modulus of subgrade reaction from FWD test
$k_{FWD-Static-Corr.}$	Static modulus of subgrade reaction from FWD test corrected for finite slab size
L	Radius of relative stiffness
LL	Liquid limit
P	Applied load
LTE	Load transfer efficiency
PI	Plasticity index
PL	Plastic limit
r	Plate radius
s_u	Undrained shear strength
w	Moisture content
w/c	Ratio of water to cement
R_t	Ratio of kinematic viscosity of permeant at temperature during time increment t_1 to t_2 to temperature of water (T)
T	Temperature
T_L	Equivalent linear temperature gradient
t_1	Time 1
t_2	Time 2
H_1	Effective head at time t_1
H_2	Effective head at time t_2
d	Effective inside diameter of standpipe
D_1	Inside diameter of bottom casing
a	+1 for impermeable base with thickness b_1 , 0 for infinite (i.e., 20 times D_1) depth of tested material, and -1 for permeable base with thickness b_1
b_1	Thickness of tested layer between bottom of device and top of underlying stratum

EXECUTIVE SUMMARY

Quality foundation layers (the natural subgrade, subbase, and embankment) are essential to achieving excellent pavement performance. Unfortunately, many pavements in the United States still fail due to inadequate foundation layers. To address this problem, a research project, Improving the Foundation Layers for Pavements (FHWA DTFH 61-06-H-00011 WO #18; FHWA TPF-5(183)), was undertaken by Iowa State University (ISU) to identify, and provide guidance for implementing, best practices regarding foundation layer construction methods, material selection, in situ testing and evaluation, and performance-related designs and specifications. As part of the project, field studies were conducted in several in-service concrete pavements across the country that represented either premature failures or successful long-term pavements. A key aspect of each field study was to tie performance of the foundation layers to key engineering properties and pavement performance. In situ foundation layer performance data, as well as original construction data and maintenance/rehabilitation history data, were collected and geospatially and statistically analyzed to determine the effects of site-specific foundation layer construction methods, site evaluation, materials selection, design, treatments, and maintenance procedures on the performance of the foundation layers and of the related pavements. A technical report was prepared for each field study.

This report summarized field test results and observations of a forensic investigation conducted on north bound (NB) and south bound (SB) lanes of NW Urbandale Drive in Urbandale, Iowa, to assess the causes of premature joint distresses observed at transverse and longitudinal joints. The SB lanes showed significantly more premature joint distresses than the NB lanes. The site consisted of a four-lane divided roadway constructed in 1997 with 260 mm (10.2 in.) thick jointed PCC pavement supported over a nominal 150 mm (5.9 in.) thick special backfill subbase layer and compacted subgrade.

Iowa State University (ISU) researchers conducted field testing on October 30 and November 7, 2013. The objectives of the field study were to assess the causes for premature joint failures on the roadway and investigate whether there were any differences between the NB and SB lanes that contributed to higher distresses on the SB lanes than on the NB lanes. The field study involved conducting falling weight deflectometer (FWD) tests on selected panels on NB and SB lanes, pavement coring near joints and away from joints, and dynamic cone penetrometer (DCP) and core hole permeameter (CHP) tests at selected core locations. FWD tests were conducted to assess load transfer efficiency (LTE) of pavement joints, deflections under dynamic loading, voids beneath pavement, and modulus of subgrade reaction (k). CHP tests were conducted to assess in situ drainage conditions. Pavement cores were assessed for damage in situ and were then sent to laboratory for petrographic analysis.

In summary, the main cause of premature joint deterioration related damage at this site is freeze/thaw distress occurring as a result of poor drainage in the joints, which has resulted in trapped water. Increased saturation because of this trapped water combined with a marginal air-void system at the surface and an elevated w/cm ratio significantly increased the risk of damage. Results obtained from NB and SB lanes did not provide conclusive evidence that there is difference between the two lanes in terms of support conditions or drainage conditions or

concrete material properties. Key findings are summarized below and followed by recommendations for partial or full depth repair.

Core Samples

- Field observations of core samples and petrographic analysis indicated that there was no significant differences between the cores obtained from NB and SB lanes. All cores showed:
 - Water-cement ratio (w/cm) ranging from about 0.45 to 0.55.
 - Air void content ranging from 4 to 7%, which is not ideal (< 5% is recommended).
 - Signs of ettringite in air voids pointing to abundant water.
- The distress observed in all the cores is consistent with freeze-thaw damage.
- Little damage was observed at the bottom of the cores except at one core location (Core 6 on NB lane). This indicates that damage is predominantly top-down, suggesting that these joints can be candidates for partial depth repairs.
- Damage appeared to be worst in samples in which the backer rod stayed where it was intended, leaving a void that was then filled with water leading to saturation and freeze-thaw distress.

Pavement Support and Drainage Conditions

Field test results are summarized in Table 4, and some key findings are as follows:

- FWD tests indicated that the average modulus of subgrade reaction value in each test section was lower than 41 kPa/mm (150 pci), which is considered “very poor” according to AASHTO (1993) design guide. The values on the SB lane were on average about 1.3 times lower than on the NB lane.
- Load transfer efficiency at joints were > 85% at most of the joints (except one), indicating good efficiency. Zero-load intercept values were all < 0.05 mm (2 mils), which indicates no voids beneath the pavements.
- CHP test results indicated that the subbase layer hydraulic conductivity varied from about 1.7E-04 to 2.8E-04 cm/s (0.5 to 0.8 ft/day) from the three test locations. No significant difference was observed between tests observed in the NB and SB lanes. The time to 50% drainage is estimated to vary from about 37 to 69 days. According to AASHTO (1993), the time for drainage > 30 days is considered to provide “very poor” drainage.

Recommendations

Prevention of future distresses in the existing concrete should focus on ensuring that water penetrating the joints is able to drain away, and to enhance the impermeability of the concrete face in the joint. This can be achieved by considering:

- Applying penetrating sealants to the face of the joints.
- Filling the joints with elastic sealant without a backer rod to avoid ponding in the kerf.
- Increasing the drainage capacity of the subbase layer.

Locations where the damage in distressed joints is confined to the top half of the slab are likely good candidates for partial depth repairs, as described by Frentress and Harrington (2012).

Locations with extensive damage will require a full depth repair. In the case of a full depth repair, the following alternative solutions are suggested:

- The current subbase layer (special backfill) provides good support with $CBR > 20$, but not adequate drainage. The drainage capacity of the subbase layer can be improved by partially replacing the existing the subbase layer with Iowa DOT 4121 granular subbase material with maximum 6% percent passing No. 200 sieve. Migration of fines from the existing subbase layer into the new subbase is possible and can be avoided by placing a geosynthetic separation layer at the interface.
- Install a geocomposite drainage layer at the interface of pavement and subbase layer. This is a relatively new application, but the concept here is that the geocompoiste drainage layer will provide an active drainage system to drain water that enters through the joints/cracks.
- Concrete mixtures should have a w/cm ratio in the range 0.40 to 0.42, with at least 5% air behind the paver. Design details should ensure that water is unable to collect and saturate joint faces.

CHAPTER 1. INTRODUCTION

Premature joint deterioration in jointed portland cement concrete (PCC) pavements is a commonly reported problem in northern United States. Recently, researchers have made efforts in determining the factors contributing to joint deterioration (Taylor et al. 2012, Jones et al. 2013, Zhang et al. 2015). Based on field investigations at multiple sites, Taylor et al. (2012) attributed the reasons for premature distresses near joints to the effectiveness of the seal in the joint, permeability in the supporting base layer, and type of aggregate used in the PCC mixture. Further, air content in the concrete less than 5%, water-to-cement (w/cm) ratio greater than 0.4, locally saturated concrete, and aggressive salting were found as critical factors that contributed to joint distresses.

In this report, results of a forensic field investigation conducted on NW Urbandale Drive in Urbandale, Iowa is presented. The site consisted of a four-lane divided roadway constructed in 1997 with 260 mm (10.2 in.) thick jointed PCC pavement supported over a nominal 150 mm (5.9 in.) thick special backfill subbase layer and compacted subgrade. The pavement experienced significant transverse joint failures along the corridor, with more severe failures along the south bound (SB) lanes than in the north bound (NB) lanes. Some longitudinal joint failures were also present. The City of Urbandale has attempted remedial patching since 2010.

Iowa State University (ISU) researchers conducted a forensic field study at the project site on October 30 and November 7, 2013. The objectives of the field study were to assess the causes of premature joint failure on the roadway and investigate whether there were any differences between the NB and SB lanes that contributed to higher distresses on the SB lanes than on the NB lanes.

The field study involved conducting falling weight deflectometer (FWD) tests on selected panels on NB and SB lanes, pavement coring near joints and away from joints, and dynamic cone penetrometer (DCP) and core hole permeameter (CHP) tests at selected core locations. FWD tests were conducted to assess load transfer efficiency (LTE) of pavement joints, deflections under dynamic loading, voids beneath pavement, and modulus of subgrade reaction (k). CHP tests were conducted to assess in situ drainage conditions. Pavement cores were assessed for damage in situ and were then sent to laboratory for petrographic analysis.

This report contains six chapters. Chapter 2 provides background information of the project. Chapter 3 presents an overview of the laboratory and in situ testing methods used in this project. Chapter 4 presents results from laboratory testing. Chapter 5 presents results from in situ testing and analysis. Chapter 6 presents key findings, conclusions, and recommendations from the study.

The findings from this report should be of significant interest to researchers, practitioners, and agencies who deal with design, construction, and maintenance aspects of PCC pavements. Results from this project provide one of several field project reports developed as part of the TPF-5(183) and FHWA DTFH 61-06-H-00011:WO18 studies.

CHAPTER 2. BACKGROUND

This chapter presents a brief literature review on joint deterioration and factors contributing to joint deterioration, following by an overview of the field project documented in this report.

Literature Review on Joint Deterioration

Premature distresses at joints in PCC pavements has been a common problem in the northern states. Taylor et al. (2011) surmised that no single mechanism can account for all forms of premature failures observed at joints, but the main contributors include freeze-thaw damage, mechanical damage, early-age damage, and D-cracking. Of all these, freeze-thaw damage is the most significant (Taylor et al. 2011).

Undrained water, the main factor contributing to freeze-thaw damage, can be present because of inadequate surface or subsurface drainage, high water table, or trapped water behind a seal above an un-cracked or non-draining joint (Weiss and Nantung 2005). Deterioration caused by freeze-thaw damage is typically first observed as shadowing with a fine network of microcracks that develop near and parallel to the joint (Figure 1). Freeze-thaw cycles open these cracks and allow more water to penetrate, which results in incremental deterioration of the joint and loss of material (Taylor et al. 2011). Concrete materials that have high saturation ($> 86\%$) will have decreased ability to resist freezing and are therefore prone to accelerated damage (Li et al. 2012). Taylor et al. (2011) summarized the following as common characteristics of frost-damaged joints:

- Pavement saturated for long periods, regardless of the source of water.
- Pavement with marginal air-void systems (total air content, spacing factors, and specific surface).
- The use of significant quantities and/or potentially aggressive deicing salts.
- Secondary ettringite deposits that fill the air-void system under saturated conditions, which indicates abundant water within the concrete.
- The damage appears as thin flakes of mortar that form parallel to the exposed surface.

Based on field investigations on multiple sites with joint deterioration in Iowa, Wisconsin, and Minnesota, Taylor et al. (2013) attributed most of the failures to the details of the system including the type and permeability of the base layer, effectiveness of the seal in the joint, and type of aggregate used in the PCC mixture. Taylor et al. (2013) concluded that almost always the failures are caused by a combination of the following factors:

- Locally saturated concrete.
- Air-void content $< 5\%$.
- Water to cement ratio (w/cm) > 0.4 .
- Aggressive salting.
- Marginal or slowly D-cracking aggregates.



Figure 1. Shadowing microcracking near joints (Taylor 2011)

Li et al. (2012) investigated the relationships between water absorption and critical saturation degree and freezing-related joint deterioration. Three groups of concrete specimens with a 0.42 w/cm ratio and volumetric air contents of 6%, 10%, and 14% were prepared and cured for 28 days. They reported that when the degree of saturation was greater than about 86%, freezing-related joint damage was found in all specimens within 1 to 6 freeze-thaw cycles. The addition of an air entraining agent significantly delayed the time for specimens to reach the critical degree of saturation from 4-6 days to 3-6 years. However, the results indicated that the addition of an air entraining agent did not reduce the potential of freezing-related joint deterioration.

Jones et al. (2013) analyzed PCC joint deteriorations and focused on freeze-thaw damage mechanisms, the use of de-icing salts, and laboratory testing results on field cores. Air void system analysis, optical microscopy analysis, freeze-thaw resistance testing, resistance to chloride ions penetration (RCP) testing, and scanning electronic microscopy (SEC) examination were conducted in laboratory on cores from field. The results indicated that concrete near deteriorated joints was always associated with poor air void systems, numerous microcracks that presented as infilling of the air voids, higher rates of absorption, high values of RCP, and low values of freeze-thaw durability factors. Use of deicing salts combined with inadequate drainage contributed to accelerated deterioration.

Zhang et al. (2015) documented results of a field study that focused on joint performance related with subsurface permeability. A core hole permeameter developed at Iowa State University was used to measure the permeability of the base material at two sealed distressed, one sealed sound, and one unsealed sound joint locations at Ames, IA. Tests were conducted in summer and winter for comparison. The base layer permeability at the sound joint was about 2 times higher than at the distressed joint in summer. In winter, the field base layer permeability was further reduced by

2 to 3 times because of frozen trapped water in the base layer. Laboratory permeability tests were conducted on the base material at various moisture contents and in frozen and unfrozen conditions. The laboratory test results confirmed the field observations of decreased permeability in frozen condition. Further, laboratory test results indicated that the permeability in both frozen and unfrozen conditions decreases as the moisture content of the material increases. Gradation analysis of the base materials under joints indicated that it contained more fines (passing the #200 sieve) than material under mid-panel. The authors attributed the reason for higher fines content at joints to material transported from the surface through the joint.

Taylor et al. (2012) documented petrographic analysis results of distressed and sound samples obtained by Zhang et al. (2015). Ettringite was observed in the distressed core sample (Figure 2), and it is indicated that the ettringite formed due to utilization of de-icing salts in winter. Some D-cracking was also found on the distressed sample. The w/cm ratio of the distressed sample was slightly greater than the sound sample.

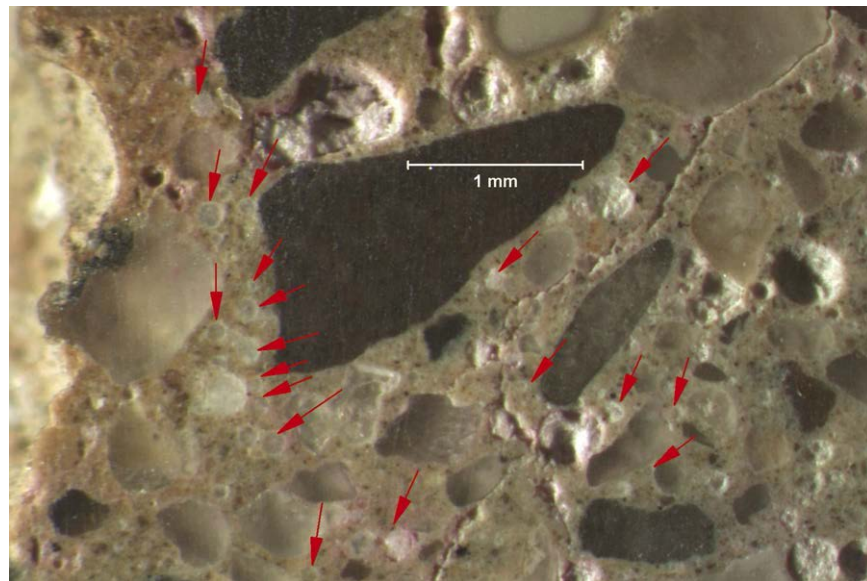


Figure 2. Petrographic examination of core sample taken from distressed joint with voids filled with ettringite at locations pointed with red arrows (Taylor et al. 2012)

NW Urbandale Drive Project Information

The project (highlighted in Figure 3) consisted of a four-lane divided roadway on NW Urbandale Drive from the I-35/I-80 bridge to just south of the Meredith Drive intersection, in Urbandale, IA. The pavement section in the corridor was originally constructed in 1997 with 260 mm (10.2 in.) thick jointed PCC pavement. According to project plans and specifications, a nominal 150 mm (5.9 in.) thick special backfill layer was placed beneath the pavement along with 300 mm (5.9 in.) deep subgrade constructed with moisture and density control. Longitudinal subdrains were installed along the outer edges of north bound (NB) and south bound (SB) lanes.

The pavement section experienced significant transverse joint failures along the corridor, specifically in the SB lanes from the interstate to the Meredith Drive intersection (Figure 4). Some longitudinal joint failures were also present. The City of Urbandale had attempted remedial patching since 2010.



Figure 3. Map of NW Urbandale Drive between I-35/I-80 ramp south of the freeway bridge to Meredith Drive in Urbandale, Iowa, with approximate locations of the test sections



Figure 4. Photos of joint deterioration observed on NW Urbandale Drive in July-August 2013 (pictures courtesy of Gary Reed, P.E. from CDA)

CHAPTER 3. EXPERIMENTAL TEST METHODS

This chapter summarizes the laboratory and in situ testing methods used in this research study.

Laboratory Testing Methods

Samples from existing subbase layers and subgrade layers were collected from the field and were carefully sealed and transported to the laboratory for testing. Particle-size analysis tests were performed on subbase layer samples in accordance with ASTM C136-06 *Standard test method for sieve analysis of fine and coarse aggregates*. Particle-size analysis tests were performed on subgrade layer samples in accordance with ASTM D422-63 *Standard test method for particle-size analysis of soils*.

Atterberg limit tests (i.e., liquid limit—LL; plastic limit—PL and plasticity index—PI) were performed in accordance with ASTM D4318-10 *Standard test methods for liquid limit, plastic limit, and plasticity index of soils* using the dry preparation method. The results from particle-size analysis and Atterberg limits tests were used to classify the materials on the unified soil classification system (USCS) in accordance with ASTM D2487-10 *Standard practice for classification of soils for engineering purposes (Unified Soil Classification System)* and AASHTO classification system in accordance with ASTM D3282-09 *Standard practice for classification of soils and soil-aggregate mixtures for highway construction purposes*.

In Situ Testing Methods and Data Analysis

Representatives from Team Services, Inc. obtained pavement cores at locations selected by representatives from CDA and ISU research team. ISU researchers examined the core samples and conducted in-situ testing. In-situ DCP and CHP tests were conducted at selected core locations. FWD tests were conducted on panels (at mid panel and joint) near the core locations. Brief descriptions of the test procedures and the field data analysis methods to estimate critical pavement design parameters are described below.

Dynamic Cone Penetrometer

DCP tests (Figure 5) were performed in accordance with ASTM D6951-03 *Standard test method for use of the dynamic cone penetrometer in shallow pavement applications*. California bearing ratio (CBR) values were determined using either Eq. 1 or 2, as appropriate, where the penetration index (PI) is in units of mm/blow.

$$CBR (\%) = \frac{292}{PI^{1.12}} \text{ for all soils with } CBR > 10 \quad (1)$$

$$CBR (\%) = \frac{1}{(0.017019 \times PI)^2} \text{ when } CBR < 10 \text{ on CL soils} \quad (2)$$

The PI of each layer was calculated as the ratio of the cumulative number of blows for each layer and the depth of the layer. These PI values were used to determine the average CBR of each layer using the equations shown above. CBR of subgrade layers is denoted as CBR_{SG} and CBR of subbase layers is denoted as CBR_{SB} in this report.



Figure 5. Dynamic cone penetrometer testing

Kuab Falling Weight Deflectometer

FWD tests were conducted using a Kuab FWD (Figure 6) setup with a 300 mm (11.81 in) diameter loading plate by applying one seating drop and three loading drops. The applied loads varied from about 27 kN (6,000 lb) to 54 kN (12,000 lb) in three loading drops. The actual applied loads were recorded using a load cell, and deflections were recorded using seismometers mounted on the device, per ASTM D4694-09 *Standard test method for deflections with a falling-weight-type impulse load device*. The FWD plate and deflection sensor setup and a typical deflection basin are shown in Figure 7. To compare deflection values from different test locations at the same applied contact stress, the values at each test location were normalized to a 40 kN (9,000 lb) applied force.

FWD tests were conducted at the center of the PCC slab panels and at the joints. Tests conducted at the joints were used to determine joint load transfer efficiency (LTE) and voids beneath the pavement based on “zero” load intercept values. Tests conducted at the center of the slab panels were used to determine modulus of subgrade reaction (k) values and the intercept values. The procedure used to calculate these parameters are described below.



Figure 6. KUAB falling weight deflectometer (FWD)

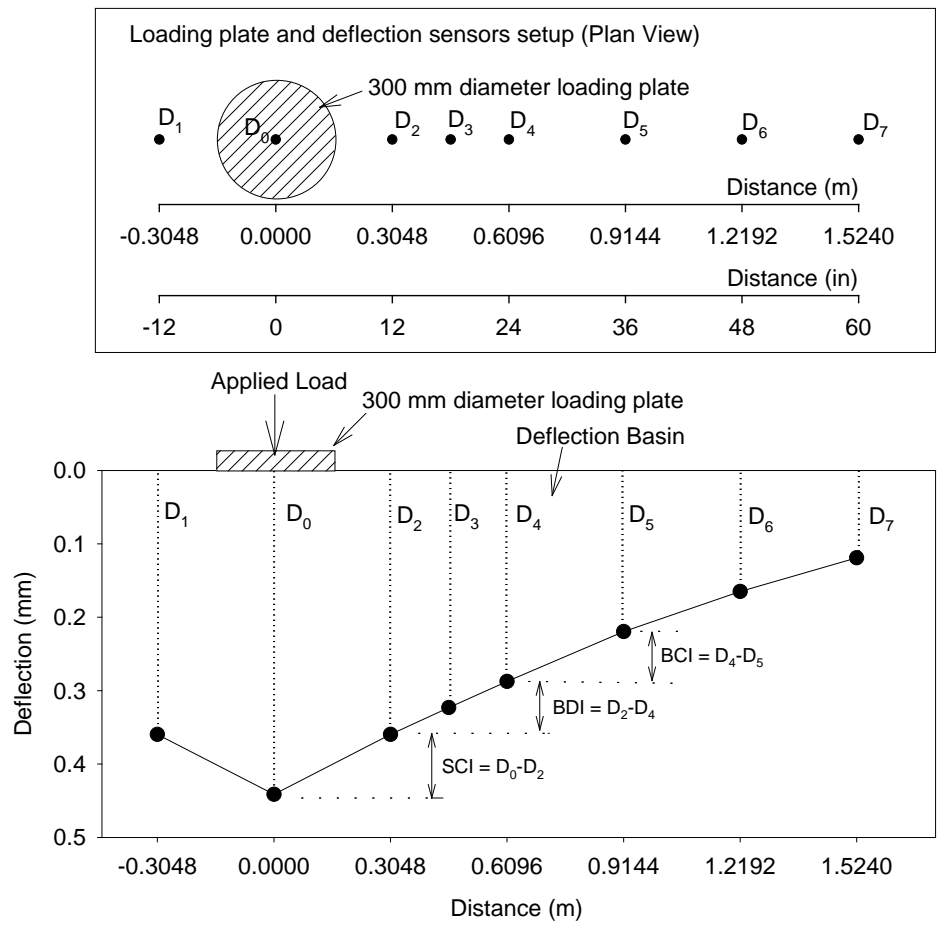


Figure 7. FWD deflection sensor setup used for this study and an example deflection basin

LTE was determined by obtaining deflections under the plate on the loaded slab (D_0) and deflections of the unloaded slab (D_1) using a sensor positioned about 305 mm (12 in.) away from the center of the plate (Figure 7). The LTE was calculated using Eq. 3:

$$LTE(\%) = \frac{D_1}{D_0} \times 100 \quad (3)$$

Voids underneath pavements can be detected by plotting the applied load measurements on the X-axis and the corresponding deflection measurements on the y-axis and plotting a best fit linear regression line, as illustrated in Figure 8, to determine the “zero” load intercept (I) values. AASHTO (1993) suggests $I = 0.05$ mm (2 mils) as a critical value for void detection. According to Quintus and Simpson (2002), if $I = -0.01$ and $+0.01$ mm, then the response would be considered elastic. If $I > 0.01$ then the response would be considered deflection hardening, and if $I < -0.01$ then the response would be considered deflection softening.

Pavement layer temperatures at different depths were obtained during FWD testing, in accordance with the guidelines from Schmalzer (2006). The temperature measurements were used to determine equivalent linear temperature gradients (T_L) following the temperature-moment concept suggested by Janssen and Snyder (2000). According to Vandenbossche (2005), I-values are sensitive to temperature induced curling and warping affects. Large positive temperature gradients (i.e., when the surface is warmer than the bottom) that cause the panel corners to curl down result in false negative I-values. Conversely, large negative gradients (i.e., when the surface is cooler than the bottom) that cause the panel corners to curl upward result in false positive I-values. Interpretation of I-values therefore should consider the temperature gradient. Concerning LTE measurements for doweled joints, the temperature gradient is reportedly not a critical factor (Vandenbossche 2005).

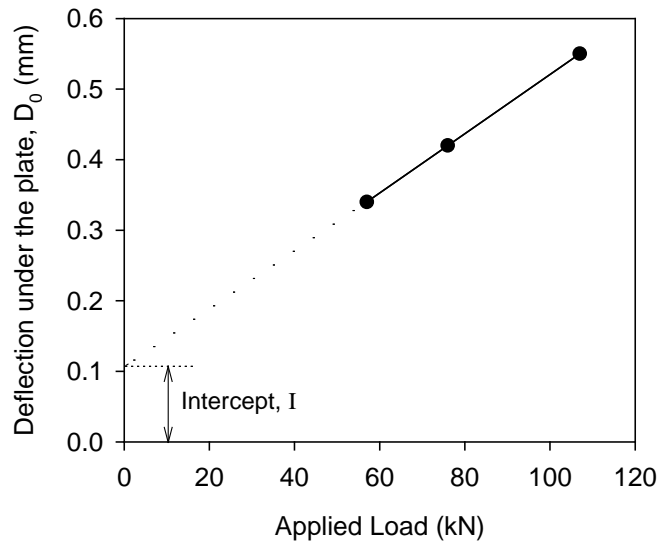


Figure 8. Void detection using load-deflection data from FWD test

The k values were determined using the AREA₄ method described in AASHTO (1993). Since the k value determined from FWD test represents a dynamic value, it is referred to here as $k_{\text{FWD-Dynamic}}$. Deflections obtained from four sensors (D_0 , D_2 , D_4 , and D_5 shown in Figure 7) were used in the AREA₄ calculation. The AREA method was first proposed by Hoffman and Thompson (1981) for flexible pavements and has since been applied extensively for concrete pavements (Darter et al. 1995). AREA₄ is calculated using Eq. 4 and has dimensions of length (in inches), as it is normalized with deflections under the center of the plate (D_0):

$$AREA_4 = 6 + 12 \times \left(\frac{D_2}{D_0} \right) + 12 \times \left(\frac{D_4}{D_0} \right) + 6 \times \left(\frac{D_5}{D_0} \right) \quad (4)$$

where D_0 = deflections measured directly under the plate (in.); D_2 = deflections measured at 305 mm (12 in.) away from the plate center (in.); D_4 = deflections measured at 610 mm (24 in.) away from the plate center (in.); and D_5 = deflections measured at 914 mm (36 in.) away from the plate center (in.). AREA method can also be calculated using different sensor configurations and setups, (i.e., using deflection data from 3, 5, or 7 sensors), and those methods are described in detail in the literature (Stubstad et al. 2006, Smith et al. 2007)

In early research conducted using the AREA method, the ILLI-SLAB finite element program was used to compute a matrix of maximum deflections at the plate center and the AREA values by varying the subgrade k , the modulus of the PCC layer, and the thickness of the slab (ERES Consultants, Inc. 1982). Measurements obtained from FWD tests were then compared with the ILLI-SLAB program results to determine the k values through back calculation. Barenberg and Petros (1991) and Ioannides (1990) proposed a forward solution procedure based on Westergaard's solution for loading on an infinite plate to replace the back calculation procedure. This forward solution presented a unique relationship between AREA value (for a given load and sensor arrangement) and the dense liquid radius of relative stiffness (L) in which subgrade is characterized by the k value. The radius of relative stiffness (L) is estimated using Eq. 5:

$$L = \left[\frac{\ln \left(\frac{x_1 - AREA_4}{x_2} \right)}{x_3} \right]^{x_4} \quad (5)$$

where $x_1 = 36$; $x_2 = 1812.279$; $x_3 = -2.559$; and $x_4 = 4.387$. It must be noted that the x_1 to x_4 values vary with the sensor arrangement and these values are only valid for the AREA₄ sensor setup. Once, the L value is known, the $k_{\text{FWD-Dynamic}}$ value can be estimated using Eq. 6:

$$k_{\text{FWD-Dynamic}} (pci) = \frac{PD_0^*}{D_0 L^2} \quad (6)$$

where P = applied load (lbs), D_0 = deflection measured at plate center (inches), and D_0^* = non-dimensional deflection coefficient calculated using Eq. 7:

$$D_0^* = a \cdot e^{-be^{-cL}} \quad (7)$$

where $a = 0.12450$, $b = 0.14707$, $c = 0.07565$. It must be noted that these equations and coefficients are valid for FWD setup with an 11.81 in. diameter plate.

The advantages of the AREA method are the ease of use without back calculation and the use of multiple sensor data. The disadvantages are that the process assumes that the slab and the subgrade are horizontally infinite. This assumption leads to underestimating the k values of jointed pavements. Croveti (1993) developed the following slab size corrections for a square slab that is based on finite element analysis conducted using the ILLI-SLAB program and is for use in the $k_{\text{FWD-Dynamic}}$:

$$\text{Adjusted } D_0 = D_0 \left(1 - 1.15085e^{-0.71878 \left(\frac{L'}{L} \right)^{0.80151}} \right) \quad (8)$$

$$\text{Adjusted } L = L \left(1 - 0.89434e^{-0.61662 \left(\frac{L'}{L} \right)^{1.04831}} \right) \quad (9)$$

where L' = slab size (smaller dimension of a rectangular slab, length or width). This procedure also has limitations: (1) it considers only a single slab with no load transfer to adjacent slabs, and (2) it assumes a square slab. The square slab assumption is considered to produce sufficiently accurate results when the smaller dimension of a rectangular slab is assumed as L' (Darter et al. 1995). Darter et al. (1995) suggested using $L' = \sqrt{\text{Length} \times \text{Width}}$ to further refine slab size corrections. However, no established procedures for correcting for load transfer to adjacent slabs have been reported so accounting for load transfer remains as a limitation of this method.

AASHTO (1993) suggests dividing the $k_{\text{FWD-Dynamic}}$ value by a factor of 2 to determine the equivalent $k_{\text{FWD-Static}}$ value. The origin of this factor 2 dates back to Foxworthy's work in the 1980's. Foxworthy (1985) reported comparisons between the $k_{\text{FWD-Dynamic}}$ values obtained using Dynatest model 8000 FWD and the Static k values (Static k_{PLT}) obtained from 30 in. diameter plate load tests (the exact procedure followed to calculate the Static k_{PLT} is not reported therein). Foxworthy used the AREA based back calculation procedure using the ILLI-SLAB finite element program. Results obtained from Foxworthy's study (Figure 9) are based on 7 FWD tests conducted on PCC pavements with slab thicknesses varying from about 10 in. to 25.5 in. and plate load tests conducted on the foundation layer immediately beneath the pavement over a 4 ft x 5 ft test area. A few of these sections consisted of a 5 to 12 in. thick base course layer and some did not. The subgrade layer material consisted of CL soil from Sheppard Air Force Base in Texas, SM soil from Seymour-Johnson Air Force Base in North Carolina, and from McDill Air

Force base in Florida (soil type was unspecified). No slab size correction was performed on this dataset.

Data from Foxworthy (1985) yielded a logarithmic relationship between the dynamic and the static k values. On average, the $k_{FWD-Dynamic}$ values were about 2.4 times greater than the Static k_{PLT} values. Darter et al. (1995) indicated that the factor 2 is reasonable based on results from other test sites (Figure 9). Darter et al. (1995) also compared FWD test data from eight long term pavement performance (LTPP) test sections with the Static k_{PLT} values and reported factors ranging from 1.78 to 2.16, with an average of about 1.91. The $k_{FWD-Dynamic}$ values used in that comparison were corrected for slab size.

For the analysis conducted in this research project, the corrected $k_{FWD-Dynamic}$ values (for finite slab size) were divided by 2 and are reported as $k_{FWD-Static-Corr}$ values.

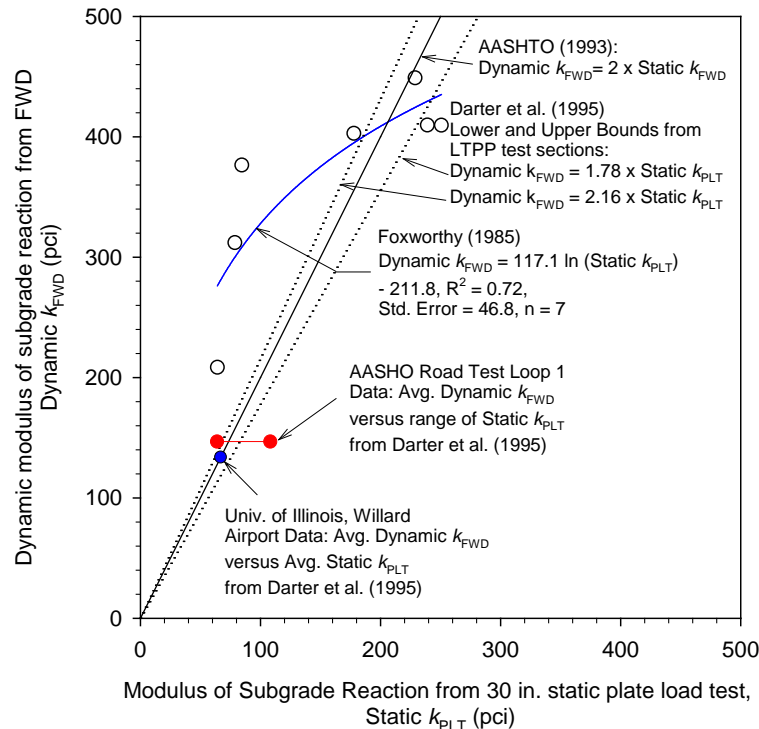


Figure 9. Static k_{PLT} values versus $k_{FWD-Dynamic}$ measurements reported in literature

Per AASHTO (1993), the subgrade layer quality ratings based on k values are as follows:

- Very good: $k > 150$ kPa/mm or 550 pci
- Good: $k = 109$ to 150 kPa/mm or 400 to 550 pci
- Fair: $k = 68$ to 95 kPa/mm or 250 to 350 pci
- Poor: $k = 41$ to 68 kPa/mm or 150 to 250 pci
- Very poor: $k < 41$ kPa/mm or 150 pci

Core Hole Permeameter

The CHP is a test device that was recently developed at ISU. The test procedure involves coring a 6 in. diameter hole in the PCC pavement down to the underlying support layer. The CHP device is inserted into the core hole and sealed at the bottom of the device and against the interior of the core hole at the bottom of the pavement. To seal the bottom of the CHP, an open cell foam ring is compressed under the CHP. By inflating a rubber tube between the outside of the CHP ring and the core-hole wall, the perimeter of the CHP is sealed against the core-hole wall. About 20 to 25 psi air pressure was used to inflate the rubber tube. Figure 10 shows the components of the CHP device and Figure 11 shows the field setup.

Tests are performed by filling the permeameter with water and recording the head loss with time for 1 minute intervals. Test readings are taken intermittently over a period of about 30 minutes (after 1, 3, 6, 10, 15, and 30 min). Determination of the hydraulic conductivity was based on concepts from ASTM D6391-06 *Standard for field measurement of hydraulic conductivity limits of porous materials using two stages of infiltration from a borehole*. For each set of readings, the water temperature was measured to correct for the viscosity of the water.



Figure 10. Core hole permeameter (CHP) device and components



Figure 11. Core hore permeability testing in situ on Urbandale Drive

The following equations were used to calculate the in situ hydraulic conductivity using the CHP (K_{CHP}).

$$K_{CHP} = \frac{R_t G_1}{t_2 - t_1} \ln \left(\frac{H_1}{H_2} \right) \quad (10)$$

$$R_t = \frac{2.2902(0.9842^T)}{T^{0.1702}} \quad (11)$$

$$G_1 = \frac{\pi a^2}{11D_1} \left[1 + \frac{aD_1}{4b_1} \right] \quad (12)$$

where, R_t = ratio of kinematic viscosity of permeant at temperature during time increment t_1 to t_2 to that of water at temperature (T) 68°F (20°C); T = temperature, H_1 = effective head at time t_1 ; H_2 = effective head at time t_2 ; d = effective inside diameter of standpipe = 1.363 in. (3.461 cm) at top and 12.985 in. (32.9816 cm) at middle; D_1 = inside diameter of bottom casing = 5 in. (12.700 cm); a = +1 for impermeable base with thickness b_1 , 0 for infinite (i.e., 20 times D_1) depth of tested material, and -1 for permeable base with thickness b_1 ; b_1 = thickness of tested layer between bottom of device and top of underlying stratum.

AASHTO (1993) provides guidance on using hydraulic conductivity values to estimate the coefficient of drainage (C_d) drainage design parameter based on pavement geometry (i.e., width of pavement, maximum distance to subdrain, cross slope, longitudinal slope); thickness of subbase layer; and effective porosity of the subbase material. The calculation involves determining the time to draining a specified percentage of water out of the pavement system. AASHTO (1993) recommends that at least 50% of drainage has occurred within the times shown in Table 1 on low-volume roads, to estimate the C_d values per Table 2. An Excel-based pavement

drainage estimator (PDE) has been developed at ISU (White et al. 2004, Vennapusa 2004) to estimate the time to 50% drainage. PDE was used for this project to determine time to 50% drainage, and estimate C_d values.

Table 1. AASHTO (1993) drainage quality rating

Quality of Drainage	Water Removed Within
Excellent	2 hours
Good	1 day
Fair	1 week
Poor	1 month
Very Poor*	(water will not drain)

*Assumed as > 30 days in estimating C_d value

Table 2. Recommended values of C_d for PCC pavement design (AASHTO 1993)

Quality of Drainage	Percent of Time Pavement Structure is Exposed to Moisture Levels Approaching Saturation			
	< 1%	1% - 5%	5% - 25%	> 25%
Excellent	1.25-1.20	1.20-1.15	1.15-1.10	1.10
Good	1.20-1.15	1.15-1.10	1.10-1.00	1.00
Fair	1.15-1.10	1.10-1.00	1.00-0.90	0.90
Poor	1.10-1.00	1.00-0.90	0.90-0.80	0.80
Very Poor	1.00-0.90	0.90-0.80	0.80-0.70	0.70

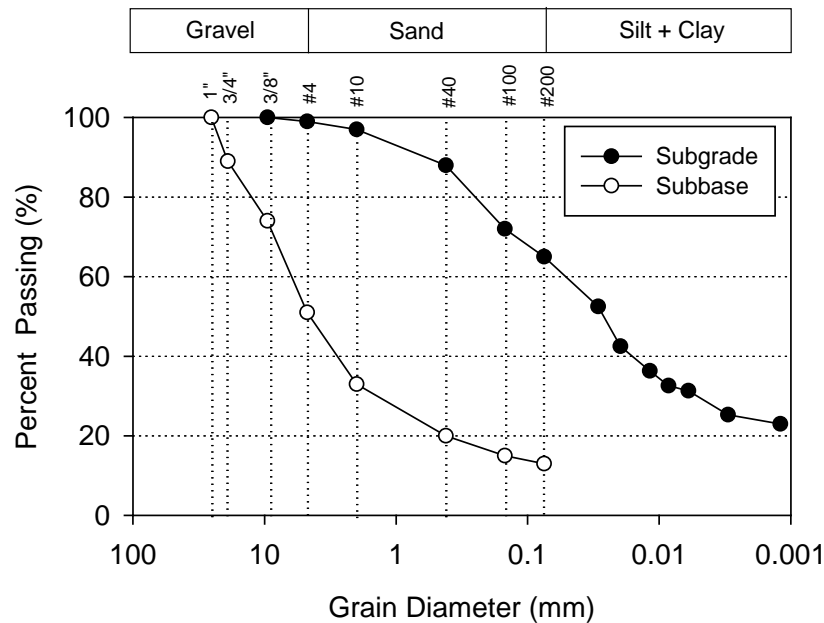
CHAPTER 4. LABORATORY TEST RESULTS

Bulk samples from subgrade and subbase layers were obtained to conduct laboratory testing to determine soil index properties. Samples were obtained from three core locations. The materials were visually similar and therefore were combined to determine the soil index properties. A summary of the material index properties (i.e., grain-size analysis, Atterberg limits test, and soil classification) is provided in Table 3. Grain-size distribution curves from particle-size analysis tests on the two materials are provided in Figure 12.

Table 3. Summary of material index properties

Parameter	Subgrade	Subbase
Gravel Content (%) (> 4.75mm)	1	49
Sand Content (%) (4.75mm – 75 μ m)	34	38
Silt Content (%) (75 μ m – 2 μ m)	42	13
Clay Content (%) (< 2 μ m)	23	13
Liquid Limit, LL (%)	46	NP
Plastic Limit, PL (%)	13	NP
Plasticity Index, PI (%)	33	NP
AASHTO Classification	A-7-6 (18)	A-1-a
USCS Classification	CL	GM

NP – Non-Plastic



CHAPTER 5. FIELD OBSERVATIONS AND TEST RESULTS

Description of Test Sections

Testing was performed on 4 test sections (TS) as summarized in Table 1. Most of the testing (TS1, TS2, and TS4) was performed on Urbandale Drive, between Meredith Drive and Plum Drive, which included FWD, CHP, and DCP testing, and 9 cores. TS3 was located north of Plum Drive, which included 1 core. FWD testing was conducted on multiple panels in each TS near joint and near mid panel, and CHP and DCP testing performed at one core location each in TS1, TS2, and TS4. Coring was performed near joints and away from joints by Team Services, Inc. In TS1 and TS2, CHP tests were conducted at core locations that were away from the joint, but in TS3, CHP tests were conducted at a core location that was located at the joint.

Cores obtained from TS2, TS3, and TS4 were sent to CTL Group for petrographic analysis. The findings from the petrographic analysis are briefly described in the following section.

Table 4. Summary of test sections and in situ testing

TS	Date	Location	In situ Tests	Comments
1	10/30/13	NB right lane on Urbandale Drive between Meredith Drive and drive way to Target Store	3 cores, 6 FWDs, 1 CHP, and 1 DCP	FWDs performed at joints and at mid-panel. DCP test performed after CHP test. 2 cores at joint and 1 core away from joint. CHP at core located away from joint.
2	11/07/13	NB right lane on Urbandale Drive just south of Plum Drive and north of drive way to Target Store	3 cores*, 12 FWDs, 1 CHP, and 1 DCP	
3	11/07/13	NB right lane on Urbandale Drive just north of Plum Drive	1 core*	—
4	11/07/13	SB right lane on Urbandale Drive, south of Plum Drive	3 cores*, 12 FWDs, 1 CHP, and 1 DCP	FWDs performed at joints and at mid-panel. DCP test performed after CHP test. 2 cores at joint and 1 core away from joint. CHP at core located at joint.

Note: FWD – falling weight deflectometer; CHP – core hole permeameter; DCP – dynamic cone penetrometer.

*Petrographic analysis performed on cores.

Core Sample Observations

The core samples were examined in the field to evaluate damage at pavement joints and assess if there were any differences between samples obtained from the NB and SB lanes. Table 5 summarizes the field observations and pictures of cores are provided in Figure 13 to Figure 18.

The distress observed in the cores is consistent with saturated freeze-thaw damage caused by undrained trapped water at the joints (in the void below backer rod) and freeze-thaw cycles.

Based on field observations of the cores, there was no difference between the cores obtained from the NB and SB lanes. The petrographic analysis report by CTL Group (Li and Jennings, 2013) supported this observation. Little damage was observed at the bottom of the cores except at Core 6, which indicates that damage is predominantly top-down. The damage appeared to be worst in core samples where the backer rod stayed where it was intended, leaving a void that was then filled with water leading to saturation and freeze-thaw distress.

Petrographic analysis indicated water-cement ratios (w/cm) ranging from about 0.45 to 0.55, signs of ettringite in air voids, and air-void contents ranging from 4 to 7% in the cores analyzed.

Table 5. Summary of core sample observations

TS	Core Number	Location	Observations
2	# 4	At joint	No damage was noticed at top or bottom of the core. Seal appeared to be missing, with backer rod at the bottom of the saw-cut and mud filled the cut (Figure 13).
	# 5	Away from joint	The core sample was in good condition (Figure 14).
	# 6	At joint	The joint was severely damaged at the surface. Visual observations indicated some distress at the bottom of the core, along with a piece of steel (Figure 15). Backer rod was located at the bottom of the saw-cut.
3	# 7	At joint	The joint was severely damaged at the surface. Some damage was observed below the saw cut (Figure 16). No damage was observed at the bottom of the core.
	# 8	Away from joint	The core was in good condition (Figure 17).
4	# 9	At joint	The joint was severely damaged at the surface. Visual observations indicated distress at the bottom of the saw-cut (Figure 18). This is typically a result of water trapped in the saw cut below the backer rod and freeze thaw cycles. Note the micro-cracking parallel to the saw face leaving flaky material, which is typically a result of freeze-thaw damage.
	# 10	At joint	The core sample was obtained from a joint that appeared to be in good condition. The core was cut through the dowel bar (Figure 19). Some damage was observed at the bottom of the saw cut similar to core # 9, but the bottom of the core did not show any damage.



Figure 13. Core 4 on NB lane south of Plum Drive (TS2)



Figure 14. Core 5 on NB lane south of Plum Drive (TS2)



Figure 15. Core 6 on NB Lane south of Plum Drive (TS2)



Figure 16. Core 7 on NB lane north of Plum Drive (TS3)



Figure 17. Core 8 on SB lane south of Plum Drive (TS4)



Figure 18. Core 9 on SB lane south of Plum Drive (TS4)



Figure 19. Core 10 on SB lane south of Plum Drive

Field Test Results

FWD test results are summarized in Figure 20 to Figure 22. Results from DCP testing are shown as DCP-CBR and cumulative blows profiles in Figure 23. Results from CHP tests from three test locations are shown in Figure 24. A summary of the field test results is provided in Table 6.

With the exception of one test location on NB lane, all joints showed $LTE > 85\%$, which generally indicates good load transfer efficiency. I values at locations were less than the critical 0.05 mm (2 mils) value, indicating no potential voids beneath the pavement. The modulus of subgrade reaction values ($k_{FWD-Static-Corr}$) varied between 37 kPa/mm (135 pci) and 46 kPa/mm (168 pci) in the NB lane and 22 kPa/mm (80 pci) and 36 kPa/mm (132 pci) in the SB lane. According to the AASHTO (1993) design guide, these values can be rated as ranging between “very poor” and “poor”. The $k_{FWD-Static-Corr}$ values obtained on the SB lane were about 1.3 times lower than obtained on the NB lane.

CHP test results indicated that the subbase layer hydraulic conductivity (K_{CHP}) varied from about 1.7E-04 to 2.8E-04 cm/s (0.5 to 0.8 ft/day) from the three test locations. No significant difference was observed between tests observed in the NB and SB lanes. Using the pavement geometry and PDE, the time to 50% drainage is estimated to vary from about 37 to 69 days. An effective porosity of 0.35 was assumed in the calculations. The estimated C_d value for time for drainage > 30 days is about 0.70 (assuming $> 25\%$ as the percent of time pavement structure is exposed to saturated conditions). According to AASHTO (1993), $C_d = 0.7$ and time for drainage > 30 days is considered “very poor”.

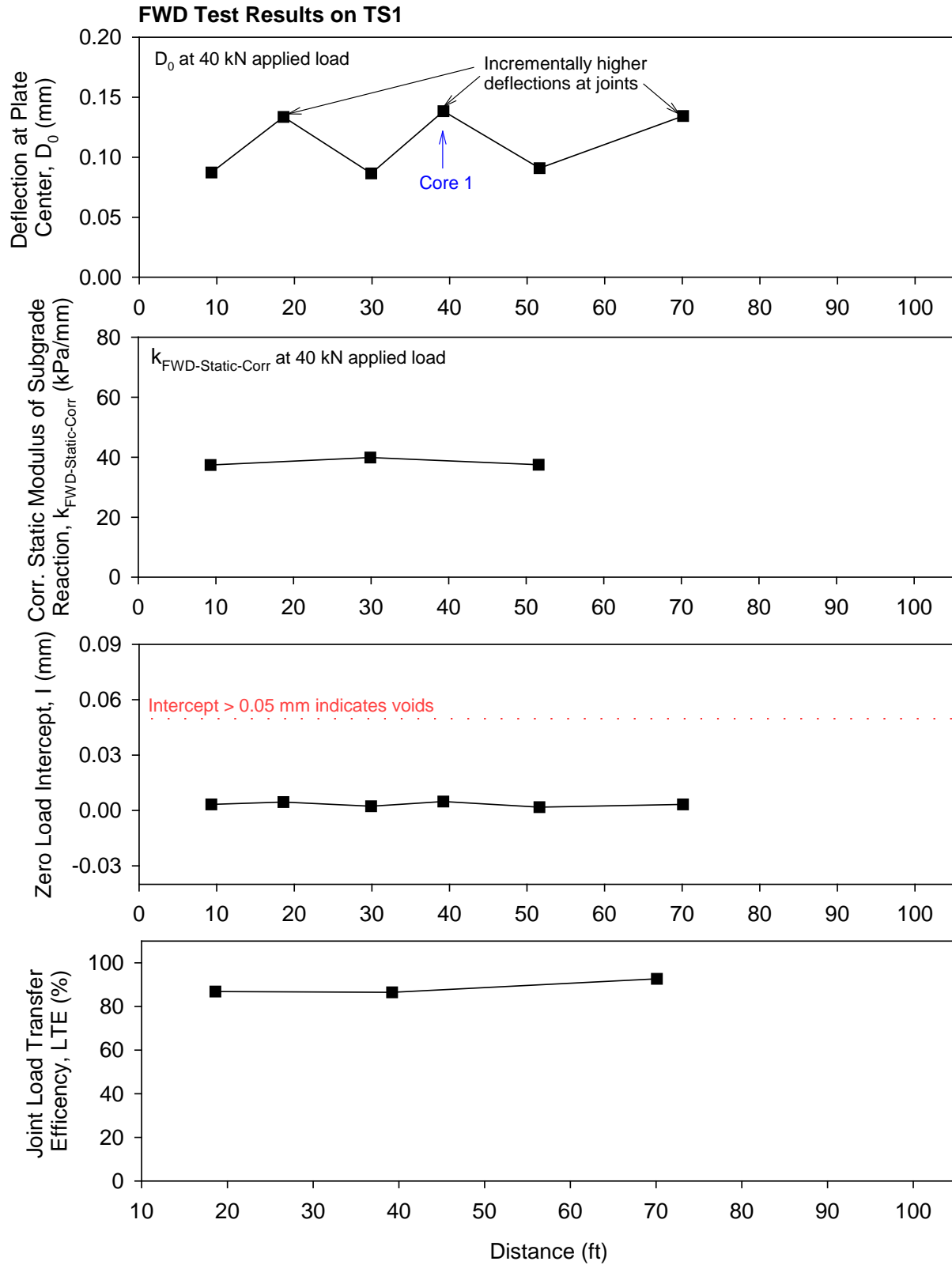


Figure 20. FWD test results from TS1

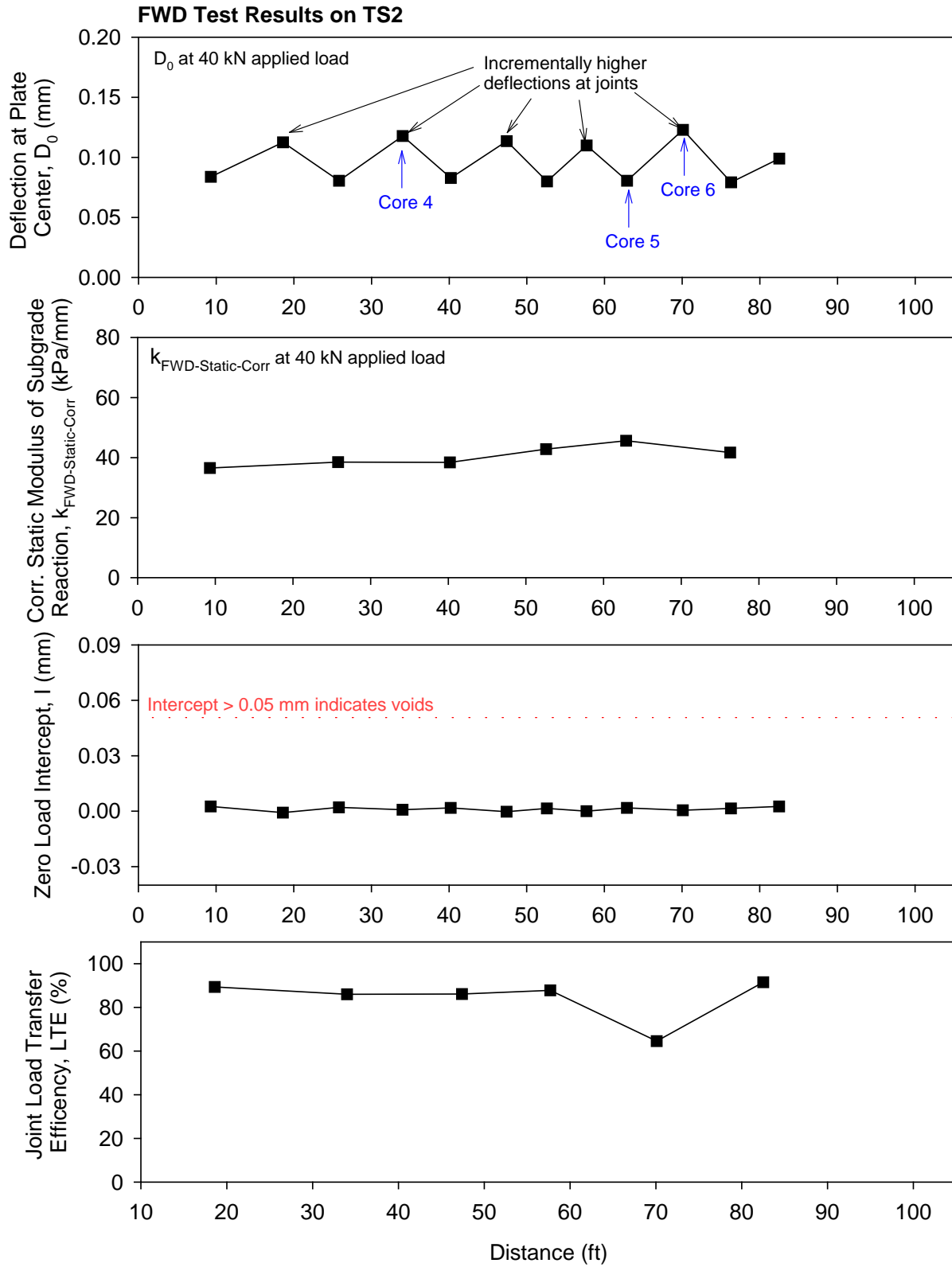


Figure 21. FWD test results on TS2

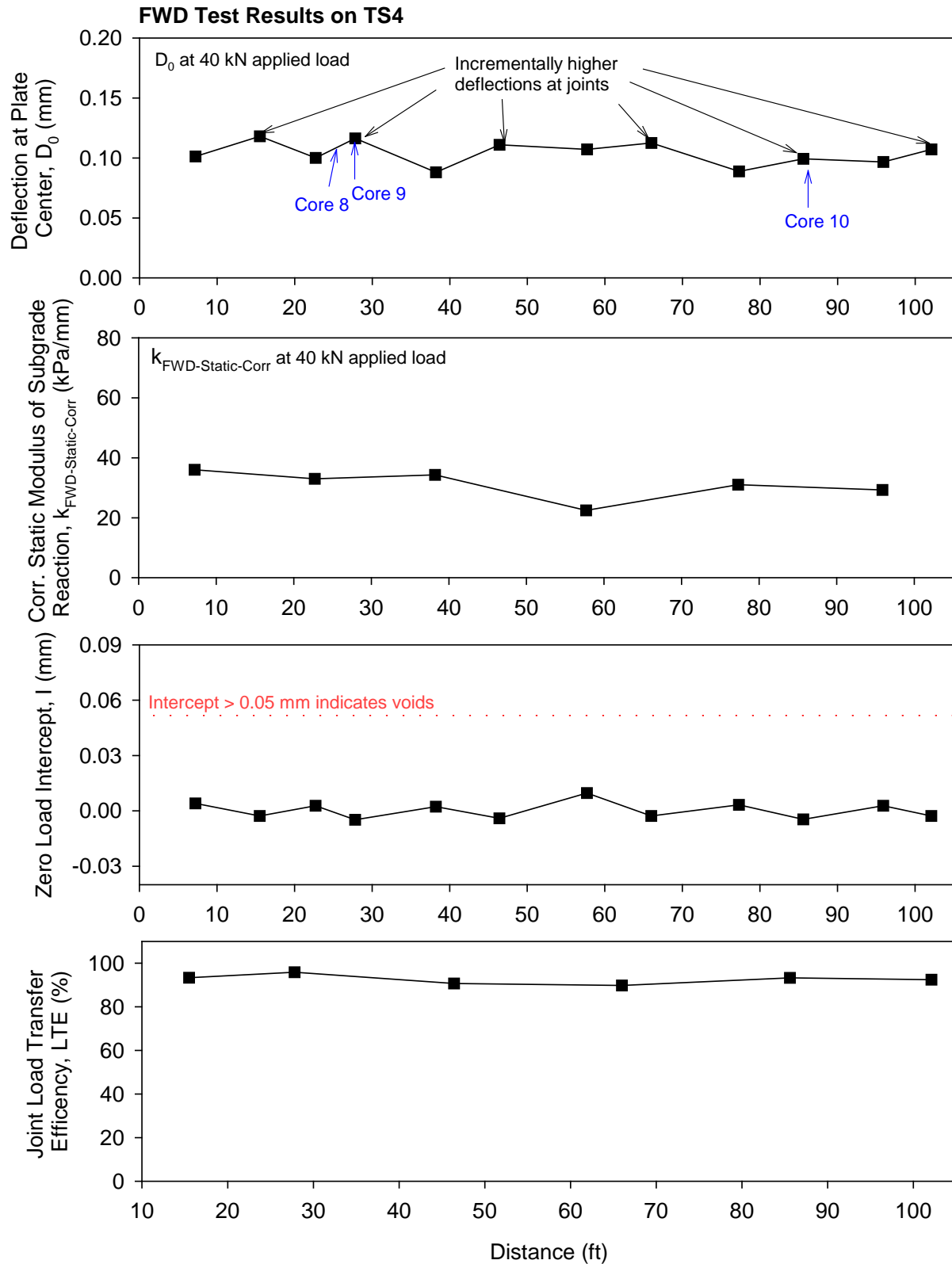


Figure 22. FWD test results from TS4

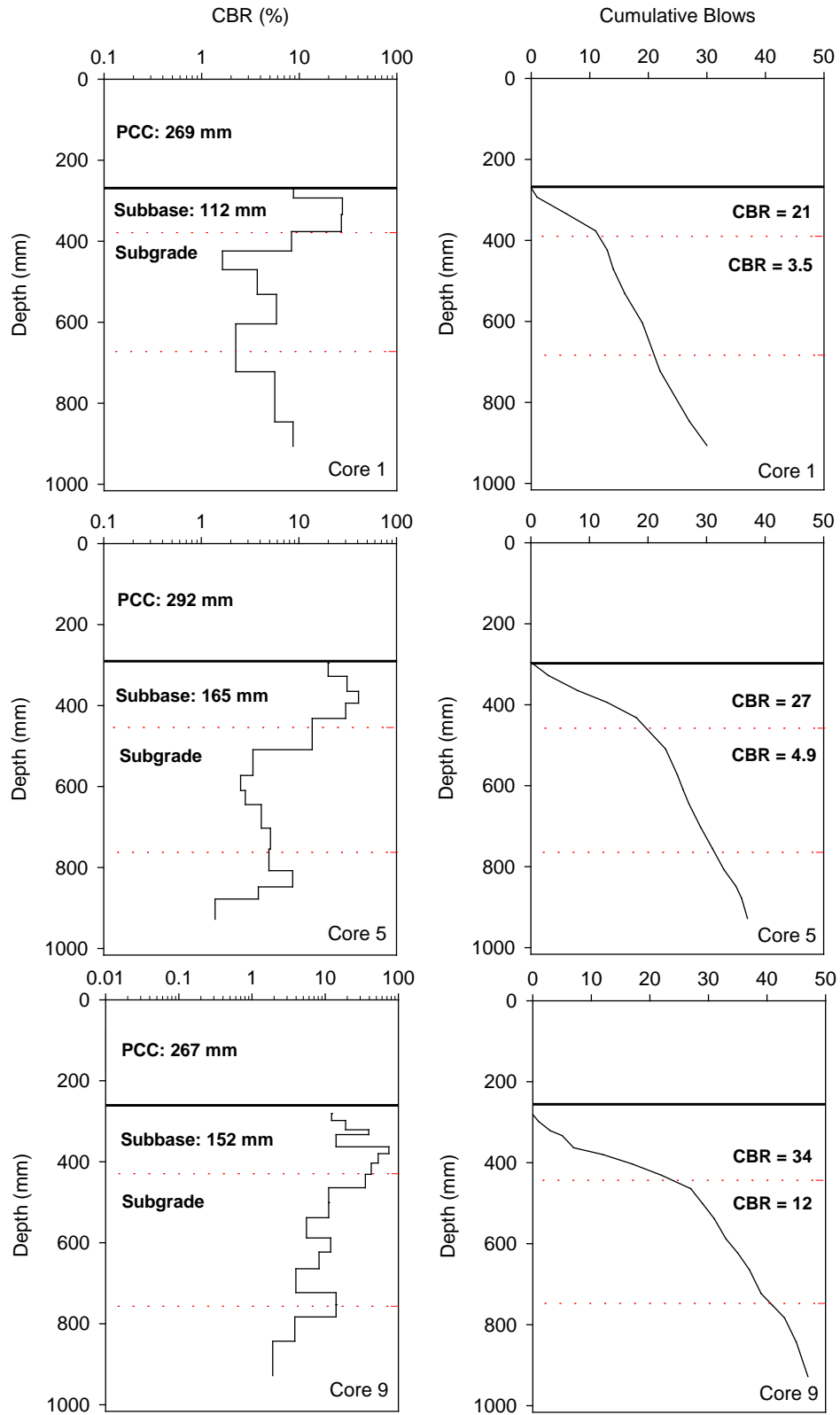


Figure 23. DCP-CBR and cumulative blows with depth from three core locations (Cores 1, 5, and 9)

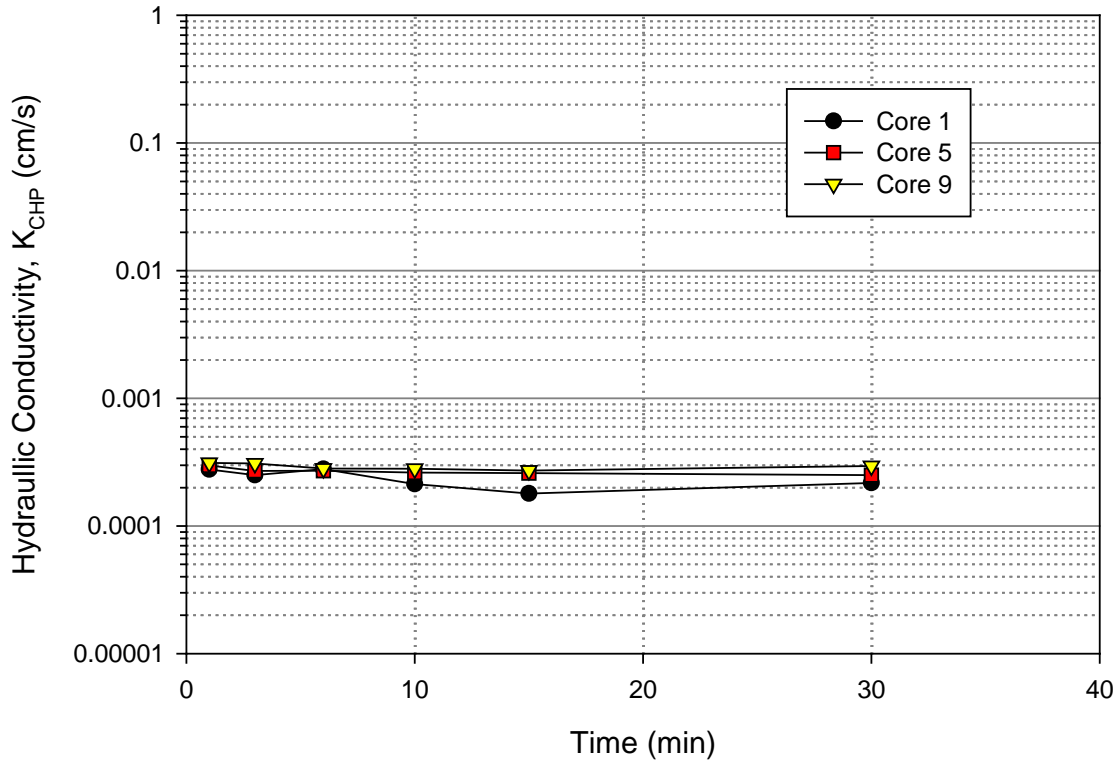


Figure 24. CHP test results from three core locations (Cores 1, 5, and 9)

Table 6. Summary of in situ test results

Measurement	TS1	TS2	TS4
Avg. D_0 (mm)	0.112	0.097	0.104
Avg. $k_{FWD-Static-Corr}$ (kPa/mm)	38.3	40.6	31.0
Avg. LTE (%)	89	84	92.6
Avg. Intercept (mm)	0.003	0.001	0.0003
CBR_{SB} (%)	21	27	34
CBR_{SG} (%)	3.7	5.1	12
K_{CHP} (cm/s)	1.8E-04	2.5E-04	2.8E-04
Time to 50% drainage (days)	69	40	37
Estimated C_d	0.70	0.70	0.70
Support quality rating based on $k_{FWD-Static-Corr}$ (AASHTO 1993)	Very Poor	Very Poor	Very Poor
Drainage quality rating (AASHTO 1993)	Very Poor	Very Poor	Very Poor

CHAPTER 6. KEY FINDINGS AND RECOMMENDATIONS

This report summarized field test results and observations of a forensic investigation conducted on NB and SB lanes of NW Urbandale Drive in Urbandale, Iowa, to assess the causes of premature joint distresses observed at transverse and longitudinal joints. The SB lanes showed significantly more premature joint distresses than the NB lanes. Field testing involved obtaining core samples for field distress evaluation and petrographic analysis, conducting FWD, DCP, and CHP testing along selected pavement panels on NB and SB lanes.

In summary, the main cause of premature joint deterioration related damage at this site is freeze/thaw distress occurring as a result of poor drainage in the joints, which has resulted in trapped water. Increased saturation because of this trapped water combined with a marginal air-void system at the surface and an elevated w/cm ratio significantly increased the risk of damage. Results obtained from NB and SB lanes did not provide conclusive evidence that there is difference between the two lanes in terms of support conditions or drainage conditions or concrete material properties. Key findings are summarized below and followed by recommendations for partial or full depth repair.

Core Samples

- Field observations of core samples and petrographic analysis indicated that there was no significant differences between the cores obtained from NB and SB lanes. All cores showed:
 - Water-cement ratio (w/cm) ranging from about 0.45 to 0.55.
 - Air void content ranging from 4 to 7%, which is not ideal (< 5% is recommended).
 - Signs of ettringite in air voids pointing to abundant water.
- The distress observed in all the cores is consistent with freeze-thaw damage.
- Little damage was observed at the bottom of the cores except at one core location (Core 6 on NB lane). This indicates that damage is predominantly top-down, suggesting that these joints can be candidates for partial depth repair.
- Damage appears to be worst in samples in which the backer rod stayed where it was intended, leaving a void that was then filled with water leading to saturation and freeze-thaw distress.

Pavement Support and Drainage Conditions

Field test results are summarized in Table 4, and some key findings are as follows:

- FWD tests indicated that the average modulus of subgrade reaction value in each test section was lower than 41 kPa/mm (150 pci), which is considered “very poor” according to the AASHTO (1993) design guide. The values on the SB lane were on average about 1.3 times lower than on the NB lane.

- Load transfer efficiency at joints were $> 85\%$ at most of the joints (except one), indicating good efficiency. Zero-load intercept values were all < 0.05 mm (2 mils), which indicates no voids beneath the pavements.
- CHP test results indicated that the subbase layer hydraulic conductivity varied from about $1.7E-04$ to $2.8E-04$ cm/s (0.5 to 0.8 ft/day) from the three test locations. No significant difference was observed between tests observed in the NB and SB lanes. The time to 50% drainage is estimated to vary from about 37 to 69 days. According to AASHTO (1993), the time for drainage > 30 days is considered to provide “very poor” drainage.

Recommendations

Prevention of future distresses in the existing concrete should focus on ensuring that water penetrating the joints is able to drain away and on enhancing the impermeability of the concrete face in the joint. This can be achieved by considering:

- Applying penetrating sealants to the face of the joints.
- Filling the joints with elastic sealant without a backer rod to avoid ponding in the kerf.
- Increasing the drainage capacity of the subbase layer.

Locations where the damage in distressed joints is confined to the top half of the slab are likely good candidates for partial depth repairs, as described by Frentress and Harrington (2012). Locations with extensive damage will require a full depth repair. In the case of a full depth repair, the following alternative solutions are suggested:

- The current subbase layer (special backfill) provides good support with $CBR > 20$, but not adequate drainage. The drainage capacity of the subbase layer can be improved by partially replacing the existing the subbase layer with Iowa DOT 4121 granular subbase material with maximum 6% percent passing No. 200 sieve. Migration of fines from the existing subbase layer into the new subbase is possible and can be avoided by placing a geosynthetic separation layer at the interface.
- Install a geocomposite drainage layer at the interface of pavement and subbase layer. This is a relatively new application, but the concept here is that the geocomposite drainage layer will provide an active drainage system to drain water that enters through the joints/cracks.
- Concrete mixtures should have a w/cm ratio in the range 0.40 to 0.42, with at least 5% air behind the paver. Design details should ensure that water is unable to collect and saturate joint faces.

REFERENCES

- AASHTO. (1993). *AASHTO design guide for design of pavement structures*. American Association of State Highway and Transportation Officials, Washington DC.
- ASTM C136-06. (2010). “Standard test method for sieve analysis of fine and coarse aggregates.” American Standards for Testing Methods (ASTM), West Conshohocken, PA.
- ASTM D422-63. (2010). “Standard test method for particle-size analysis of soils.” American Standards for Testing Methods (ASTM), West Conshohocken, PA.
- ASTM D2487-10. (2010). “Standard test method for classification of soil for engineering purposes (unified soil classification system).” American Standards for Testing Methods (ASTM), West Conshohocken, PA.
- ASTM D3282-09. (2010). “Standard test method for classification of soils and soil-aggregate mixtures for highway construction purposes.” American Standards for Testing Methods (ASTM), West Conshohocken, PA.
- ASTM D4318-10. (2010). “Standard test methods for liquid limit, plastic limit, and plasticity index of soils.” American Standards for Testing Methods (ASTM), West Conshohocken, PA.
- ASTM D4694-09. (2009). “Standard test method for deflections with a falling-weight-type impulse load device.” American Standards for Testing Methods (ASTM), West Conshohocken, PA.
- ASTM D6391-06. (2006). “Standard test method for field measurement of hydraulic conductivity limits of porous materials using two stages of infiltration from a borehole.” American Standards for Testing Methods (ASTM), West Conshohocken, PA.
- ASTM D6951-03 (2010). “Standard test method for use of the dynamic cone penetrometer in shallow pavement applications.” American Standards for Testing Methods (ASTM), West Conshohocken, PA.
- Crovetti, J. A. (1994). “Evaluation of jointed concrete pavement systems incorporating open-graded bases.” Ph.D. Dissertation, University of Illinois at Urbana-Champaign, IL.
- Darter, M. I., Hall, K. T., and Kuo, C-M. (1995). *Support under Portland Cement Concrete Pavements*, NCHRP Report 372, Transportation Research Board, Washington, D.C.
- ERES Consultants Inc. (1982). *Techniques for Pavement Rehabilitation: A Training Course*. U.S. Department of Transportation, FHWA, Washington, D.C.
- Foxworthy, P. T. (1985). “Concepts for the Development of a Nondestructive Testing and Evaluation System for Rigid Airfield Pavements.” Ph.D. Thesis, University of Illinois at Urbana-Champaign, IL.
- Frentress, D., and Harrington, D. S. (2012). *Guide for Partial Depth Repair of Concrete Pavements*, National Concrete Pavement Technology Center, Iowa State University, Ames, IA.
- Hoffman, M. S., and Thompson, M. R. (1981). *Mechanistic Interpretation of Nondestructive Pavement Testing Deflections*. Transportation Engineering Series No. 32, Illinois Cooperative Highway and Transportation Research Series No. 190, University of Illinois at Urbana-Champaign, Champaign, IL.
- Jones, W., Farnam, Y., Imbrock, P., Spiro, J., Villani, C., Golias, M., Olek, J., Wiess, J. W. (2013). *An overview of joint deterioration in concrete pavement: Mechanisms, solution properties, and sealers*, Purdue University, West Lafayette, IN.

- Ioannides, A. M. (1990). "Dimensional analysis in NDT rigid pavement evaluation," *Transportation Engineering Journal*, ASCE, Vol. 116, No. TE1.
- Jannsen, D., and Snyder, M. (2000). Temperature-Moment Concept for Evaluating Pavement Temperature Data. *Journal of Infrastructure Systems*, 6(2), 81–83.
- Li, Q., and Jennings, V. A. (2013). *Petrographic Examination of Concrete Cores from NW Urbandale Drive, Urbandale, Iowa*, CTL Group Project No. 150742, Report prepared for Team Services, Inc., CTL Group, Skokie, IL.
- Li, W., Pour-Ghaz, M., Castro, J., Wiess, J. (2012). "Water absorption and critical degree of saturation relating to freeze-thaw damage in concrete pavement joints," *Journal of Materials in Civil Engineering*, 24(3), 299–307.
- Quintus, V. H. L., and A. L. Simpson. (2002). *Backcalculation of Layer Parameters for LTPP Test Sections, Volume II: Layered Elastic Analysis for Flexible and Rigid Pavements, Research Report, Long-Term Pavement Performance Program*, Report No. FHWA-RD-01-113, Federal Highway Administration, Washington, D.C., October 2002.
- Schmalzer, P. (2006). *LTPP Manual for Falling Weight Deflectometer Measurements—Version 4.1* (Report No. FHWA-HRT-06-132). Washington, D.C.: Federal Highway Administration.
- Smith, K. D., Wade, M. J., Bruinsma, J. E., Chatti, K., Vandenbossche, J. M., Yu, H. T., Hoerner, T. E., Tayabji, S. D. (2007). *Using Falling Weight Deflectometer Data with Mechanistic-Empirical Design and Analysis*, Draft Interim Report, DTFH61-06-C-0046, Federal Highway Administration, Washington, D.C.
- Substad, R. N., Jiang, Y. J., and Lukanen, E. O. (2006). *Guidelines for Review and Evaluation of Backcalculation Results*, FHWA-RD-05-152, Federal Highway Administration, Washington, D.C.
- Taylor, P. C. (2011). "Preventing joint deterioration in concrete pavements: A summary of current knowledge," MAP Brief 6-1, Road Map Track 6, CP Road Map.
- Taylor, P. C., Rasmussen, R. O., Torres, H., Fick, G., Harrington, D., Cackler, E. T. (2011). *Interim Guide for Optimum Joint Performance of Concrete Pavements*, Ames IA, National Concrete Pavement Technology Center, 2nd Edition, July 2012.
- Taylor, P. C., Sutter, L., Weiss, J. (2012). *Investigation of deterioration of joints in concrete pavements*, DTFH61-06-H-0011 Work Plan 26, InTrans Project 09-361, National Concrete Pavement Technology Center, Iowa State University, Ames, IA.
- Vandenbossche, J. M. (2005). "Effects of slab temperature profiles on the use of falling weight deflectometer data to monitor joint performance and detect voids." *Transportation Research Record: Journal of the Transportation Research Board*, 2005, 75–85.
- Vennapusa, P. (2004). *Determination of Optimum Base Characteristics for Pavements*, MS Thesis, Iowa State University, Ames, IA.
- White, D. J., Vennapusa, P., Jahren, C. T. (2004). *Determination of the Optimum Base Characteristics for Pavements*, Iowa DOT Project TR-482, Iowa Highway Research Board, Iowa Department of Transportation, Ames, IA.
- Zhang, J., White, D. J., Taylor, P. C., Shi, C. (2015). "A case study of evaluation joint performance in relation with subsurface permeability in cold weather region," *Cold Regions Science and Technology*, 110, 19–25.